Miscibility, Crystallization, and Melting of the Blends of a Ferroelectric VDF/TrFE Copolymer and PMMA

KAP JIN KIM,* GWAN BUM KIM, and SEUNG HWA HAN

Department of Textile Engineering, College of Engineering, Kyung Hee University, #1 Seochun-ri, Kiheung-eup, Yongin-kun, Kyunggi-do 449-701, South Korea

SYNOPSIS

Factor analysis by IR and melting-point depression indicated miscibility between poly(vinylidene fluoride/trifluoroethylene) [P(VDF/TrFE)] and poly(methyl methacrylate) (PMMA) in the melt state. χ_{12} was found to be −0.229 at 160°C. PMMA reduced the rate of crystallization of P(VDF/TrFE) drastically by increasing both ΔG^* and ΔG_η. The double melting of the blend crystallized nonisothermally originated from the presence of two morphologically different crystals in the paraelectric crystalline state. © 1993 John Wiley & Sons, Inc.

INTRODUCTION

The crystalline morphology, crystallization kinetics, miscibility, and melting behavior of miscible blends of poly(vinylidene fluoride) (PVDF)/poly(methyl methacrylate) (PMMA), in which PVDF is crystallizable and PMMA is amorphous, have been extensively investigated.[1†] Miscibility between PVDF and PMMA was elucidated by IR[2] and melting-point depression.[1†] As the concentration of amorphous PMMA increases, the thickness of the folded-chain lamellae becomes thinner and the rate of crystallization slows down dramatically. But there have been only a few studies[3] on the blends of PMMA and random copolymers of vinylidene fluoride (VDF) and trifluoroethylene (TrFE) having physicochemical properties similar to PVDF. The main purpose of this paper is to analyze miscibility in the melt state by IR and melting-point depression, the effect of amorphous PMMA on the crystallization behavior of P(VDF/TrFE), and the origin of melting-point depression and double melting in the blends of P(VDF/TrFE) and PMMA. The effect of PMMA on ferroelectric properties of P(VDF/TrFE) was discussed in a separate paper.[4]

EXPERIMENTAL

Random copolymer of VDF and TrFE samples with a molar ratio of 75/25 have been obtained from Pennwalt Corporation and *atactic* PMMA with medium molecular weight (inherent viscosity = 0.45) has been purchased from Aldrich Chemical Co. Films of P(VDF/TrFE), PMMA, and their mixtures were cast from 5% acetone solution onto glass plates, quickly transferred to the drying oven maintained at 50°C, dried for 1 h, and further dried under vacuum for 24 h. The IR absorbance spectra of blends in the melt state were recorded at 180°C using a Nicolet MX-1 spectrometer with a resolution of 2 cm^{-1} and 32 scans. All the IR data were transferred to a personal computer interfaced to the IR spectrometer. Factor analysis was performed on the absorbance data of all the mixtures in the range of 1800–800 cm^{-1}. Isothermal crystallization at small undercoolings was performed on a Nikon polarized microscope equipped with a Mettler FP82HT hot stage and a photosensor under the crossed nicoles. The electrical signals as a function of time for changes in light intensity during crystallization were transferred to a personal computer and saved in the magnetic disc for further analysis. To prepare samples for the measurement of equilibrium melting temperature, samples were maintained at 180°C for 10 min, subsequently quenched to a desired temperature, and then crystallized isothermally for 3 h

* To whom correspondence should be addressed.

† Refs. 1–14 in Ref. 1.

Journal of Applied Polymer Science, Vol. 49, 7–13 (1993)
 CCC 0021-8995/93/010007-07

on DSC and cooled to room temperature. The melting endotherms of isothermally crystallized samples were obtained by heating at a rate of 10°C/min on a Perkin-Elmer DSC-IV that was calibrated with indium. Melting temperature was obtained from the peak temperature of the melting endotherm. Nonisothermal crystallization was also measured on the same differential scanning calorimeter at various cooling rates (2, 4, 8, 16, 30, 60°C/min).

RESULTS AND DISCUSSION

Figure 1 shows the absorbance spectra of P(VDF/TrFE) and PMMA blends in the melt state. One can rarely find a significant shift or new band in the spectra attributed to the specific intermolecular interaction as a function of composition only with spectra themselves. More sophisticated examination such as factor analysis is needed to elucidate the specific interaction between these two polymers in the melt state. The specific intermolecular interaction between two polymers in the binary mixture results in the shift of absorption bands or new absorption peaks, and factor analysis of IR spectra is often used to evaluate the miscibility of polymer blends. Factor analysis can allow one to determine the number of linearly independent components of a blend system. If the *trans/gauche* ratio is different in pure P(VDF/TrFE) and in P(VDF/TrFE) mixed with PMMA, as in the case of a PVDF/PMMA blend system,[2] and/or new absorption peaks attributed to PMMA intermolecularly interacted with P(VDF/TrFE) are created, the absorbance spectra of the blends can be expressed in a linear combination of at least three or four components. Factor analysis was performed on the absorbance spectra in the conformation- and specific interaction-sensitive region 1800–800 cm^{-1}. The results of factor analysis of the IR spectra of P(VDF/TrFE)/PMMA blends of various PMMA compositions in the melt state are shown in Table I. The number of factors found in this binary mixture on the basis of the Malinowski's IND criterion was four.[5] The first two components can be naturally identified as P(VDF/TrFE) and PMMA; the third may be due to PVDF conformational changes induced by interaction, and the fourth, to new absorption peak or peak shift of PMMA originating from intermolecular interaction between them. On the contrary, in the miscible PVDF/PMMA blend system in the melt state, they reported that there

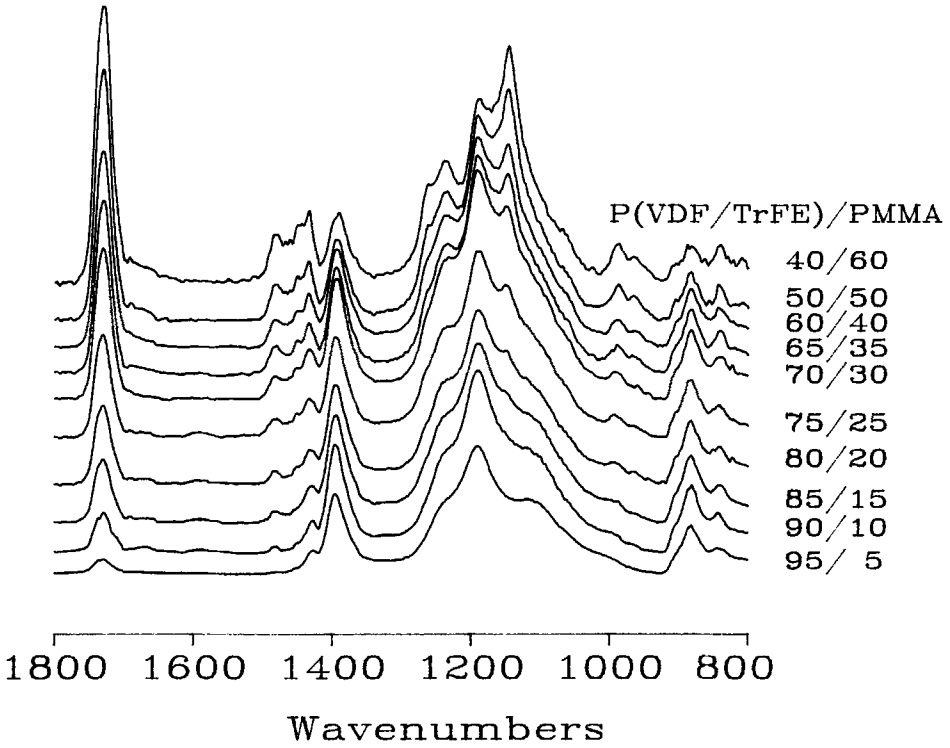

Figure 1 IR absorbance spectra of P(VDF/TrFE)/PMMA blends in the melt state, i.e., at 180°C.

Table I Factor Analysis of FTIR Spectra of P(VDF/TrFE)/PMMA Blends in the Region of 1800 to 800 cm^{-1}

Eigenvalue	Log(Eigenvalue)	RE × 10^4	IND × 10^4
9.864220	0.994064	38.12	0.4706
0.131129	−0.882301	7.49	0.1170
0.003189	−2.496246	4.50	0.0918
0.001173	−2.930576	2.18	0.0608
0.000134	−3.871070	1.77	0.0710
0.000077	−4.110931	1.44	0.0901
0.000037	−4.430611	1.25	0.1398
0.000024	−4.612069	1.09	0.2739
0.000018	−4.744335	0.81	0.8159
0.000006	−5.160391	—	—

were only three factors[2]: They identified the first two components as PVDF and PMMA and the third to be due to PVDF conformational changes induced by interaction. The choice of the narrow region 1320–930 cm^{-1}, which is much more sensitive to the conformational change of PVDF than to that of PMMA, might have shown only three factors. Taking the PMMA-sensitive region into consideration would also have given four factors. The present result of factor analysis indicates that the specific interaction between P(VDF/TrFE) and PMMA in the melt state exists and that these two polymers are miscible as in the case of the PVDF/PMMA mixture.

The equilibrium melting point of a miscible blend, in which one component is crystallizable and the other is amorphous, is continuously depressed at higher concentrations of the amorphous component. The polymer–polymer interaction parameter (χ_{12}) can be calculated by eq. (1) given by Nishi and Wang[6]:

$$\frac{1}{T_m} - \frac{1}{T_m^0} = -\frac{RV_{2u}}{\Delta h_{2u} V_{1u}} \chi_{12} \phi_1^2 \qquad (1)$$

where T_m^0 and T_m are the equilibrium melting points of P(VDF/TrFE) and the blend, respectively; V_{1u} and V_{2u}, the molar volume of PMMA (83.3 cm^3/mol) and P(VDF/TrFE) (37.1 cm^3/mol), respectively; Δh_{2u}, the heat of fusion of P(VDF/TrFE) (1425 cal/mol); ϕ_1, the volume fraction of PMMA; and R, the gas constant.

The equilibrium melting points of the blends were obtained from a Hoffman–Weeks plot and χ_{12}, determined according to eq. (1), was found to be −0.229 at 160°C. Comparison of this value with the corresponding values for the PVDF/PMMA blend (χ_{12} = −0.295 at 160°C)[6] and the P(VDF/TrFE) (78.5/21.5)/PMMA system (χ_{12} = −0.261 at 150°C)[4] shows that the system with higher TrFE composition has a smaller negative value, suggesting that the present system may be less compatible than are the other two.

The melting-point depression may be related to the crystalline morphology as well as to the thermodynamic interaction, and it has been reported that the interaction parameter may not be a constant but may depend on concentration.[1,7‡] Considering a two-dimensional nucleation and chain-folding crystallization, Chow[1] modified eq. (1), incorporating the effects of both crystalline morphology and thermodynamic interaction as

$$\frac{T_m}{T_m^0} = 1 - \frac{2\gamma_e}{l\Delta h_{2u}} + \frac{RT_m}{V_{1u}\Delta h_{2u}} \chi_{12} \phi_1^2 \qquad (2)$$

where γ_e is the surface free energy per unit area for the fold surface in chain-folded lamellar crystal and l is the lamellar thickness. According to Chow's procedure, l and χ_{12} were determined as follows:

$$1/l = a \cdot \Delta h_{2u}(1 - \phi_c)\phi_1^2/(2\gamma_e) \qquad (3)$$

and

$$\chi_{12} = -a \cdot V_{1u}\Delta h_{2u}\phi_c/(RT_m) \qquad (4)$$

where

$$a = (T_m^0 - T_m)/(T_m^0 \phi_1^2) \qquad (5)$$

and ϕ_c is the measured degree of crystallinity, which can be expressed in the form

$$\phi_c = \phi_c^0 - \beta\phi_1^2 \qquad (6)$$

Figure 2 shows melting temperature and degree of crystallinity as a function of volume fraction of PMMA (ϕ_1) for samples crystallized on a Mettler FP82HT hot stage at the identical degree of undercooling (20°C) until no further increase of light intensity was observed. The melting endotherms of these isothermally crystallized samples were obtained by rescanning them at a rate of 10°C/min on a Perkin-Elmer DSC-IV after cooling them to room temperature. Melting temperature was obtained from the peak temperature of the melting endotherm and the degree of crystallinity was calculated from the melting enthalpy. The values of a,

‡ Refs. 12–17 in Ref. 1.

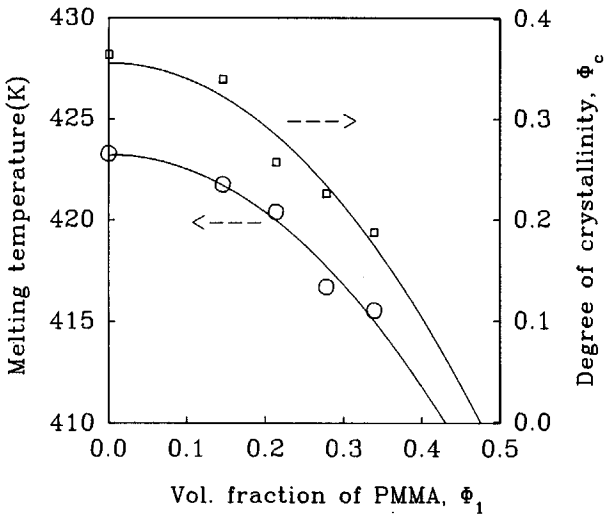

Figure 2 Plots of melting temperature and degree of crystallinity vs. volume fraction of PMMA.

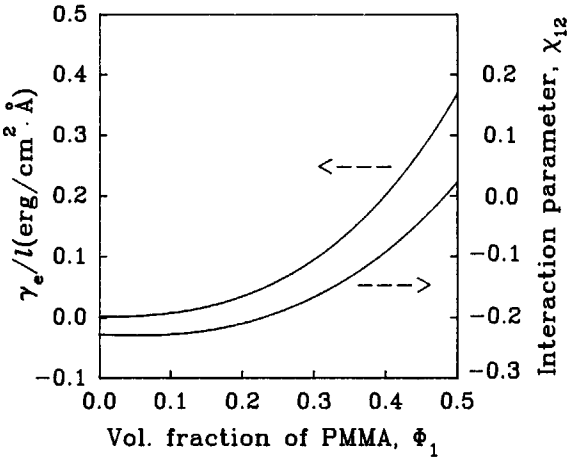

Figure 3 Concentration-dependent lamellar thickness and interaction parameter in the P(VDF/TrFE)/PMMA system.

T_m^0, β, and ϕ_c^0 were calculated from Figure 2 by curve-fitting based on eqs. (5) and (6). All parameters for Chow's thermal analysis are listed in Table II.

Figure 3 shows the dependence of P(VDF/TrFE) crystal thickness l and interaction parameter χ_{12} at 160°C on the volume fraction of PMMA. The thickness of lamella becomes smaller and χ_{12} attains a smaller negative value at a higher concentration of amorphous PMMA. The plot of χ_{12} vs. ϕ_1 for the P(VDF/TrFE)/PMMA system is located higher than the corresponding plot for the PVDF/PMMA system reported by Chow.[1] This result also indicates that the present blend system may be less compatible than is the PVDF/PMMA system.

Figure 4 shows the inverse of the crystallization half-time, $(t_{1/2})^{-1}$ vs. the degree of undercooling. The rate of crystallization is reduced drastically with an increase of PMMA in the blend. The presence of a miscible amorphous PMMA is expected to have a strong effect on the rate of crystallization of P(VDF/TrFE) in the P(VDF/TrFE)/PMMA system. $(t_{1/2})^{-1}$ can be expressed by a modified Turnbull–Fisher equation[8]:

$$(t_{1/2})^{-1} = A_0 \exp[-(\Delta G_\eta + \Delta G^*)/kT] \quad (7)$$

where A_0 is a constant that is compositionally dependent; k, a Boltzmann constant; ΔG_η, the acti-

Table II Parameters for Thermal Analysis of P(VDF/TrFE)/PMMA Blends by Chow's Procedure[1]

V_{1u} (cm^3/mol)	83.3	
V_{2u} (cm^3/mol)	37.1	
Δh_{2u} (cal/cm^3)	38.3	
T_m° (K)	423.2[a]	431.2[b]
a	0.1682	
ϕ_c°	0.3554	
β	1.5728	

[a] This is not true equilibrium melting point of pure P(VDF/TrFE), but the measured melting point of P(VDF/TrFE) crystallized at 138°C on a Mettler hot stage until no change in the transmitted light intensity is observed.

[b] From a Hoffman–Weeks plot.

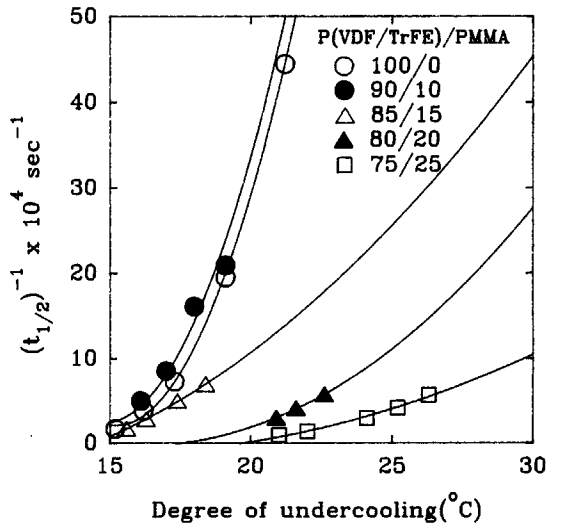

Figure 4 Plots of $(t_{1/2})^{-1}$ vs. the degree of undercooling for the P(VDF/TrFE)/PMMA system.

vation energy for the diffusion of the crystallizing segment across the phase boundary; and ΔG^*, the free energy of crystallization of the nucleus of critical size. Since $\Delta G_\eta/kT$ can be expressed as $C_1/(C_2 + T - T_g)$,[1,8] $\Delta G_\eta/kT$ can be regarded to be constant if the variation in the crystallization temperature is not large at low undercooling. Thus, eq. (7) can be rewritten as

$$(t_{1/2})^{-1} = A_1 \exp(-\Delta G^*/kT) \quad (8)$$

or

$$\ln t_{1/2} = A_2^* + \Delta G^*/kT \quad (9)$$

Considering a two-dimensional nucleation process involving the monomolecular deposition of chain units on the crystal surface, ΔG^* can be expressed as[8]

$$\Delta G^* = 4b_0\gamma\gamma_e T_m/(\Delta h_f \Delta T \rho_c) \quad (10)$$

where b_0 is the molecular thickness; γ and γ_e, the surface energy per unit area of the side and end surfaces of nucleus (cm^2/erg), respectively; T_m, the equilibrium melting point; Δh_f, the heat of fusion per unit weight of bulk crystal (erg/g); ΔT, the degree of undercooling; and ρ_c, the density of the bulk crystal (g/cm^3). Combination of Eqs. (9) and (10) yields eq. (11):

$$\ln t_{1/2} = A_2 + 4b_0\gamma\gamma_e T_m/(\Delta h_f \Delta T \rho_c kT) \quad (11)$$

Thus, $\gamma\gamma_e$ can be calculated from the slope of the plot of $\ln t_{1/2}$ vs. $1/(\Delta T \cdot T)$. In calculating the value of the $\gamma\gamma_e$, the values of the various constants have been taken as $\Delta h_f = 8.708 \times 10^8$ erg/g, $\rho_c = 1.8455$ g/cm^3, and $b_0 = 4.45 \times 10^{-8}$ cm. The results are listed in Table III. The calculated value of $\gamma\gamma_e$ is very close to that for the PVDF/PMMA system as reported by Chow,[1] but it is half that for the PVDF/PMMA blend as reported by Wang and Nishi.[9] ΔG^* increases slightly with an increase in PMMA composition, which is consistent with the PVDF/PMMA system.[9] The value of ΔG_η also increases with the addition of PMMA. Thus, the reduction of the rate of crystallization in the P(VDF/TrFE)/PMMA blend may be attributed to an increase in the magnitudes of both ΔG^* and ΔG_η. The constant A_0 in eq. (7), which may reflect the concentration of the crystallizable component at the crystal growth front and the rate at which the amorphous component is removed from the growth front, can be expected to have a reduced value with an increase in PMMA composition.

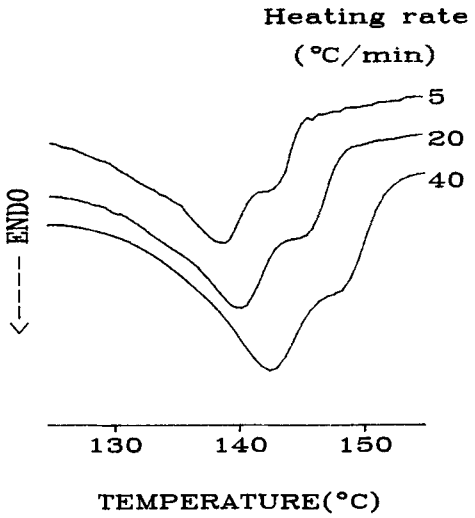

Figure 5 DSC melting transition curves with various heating rates for the P(VDF/TrFE)/PMMA (80/20) blend crystallized nonisothermally from the melt to 10°C at −10°C/min.

Table III Thermodynamic Parameters for Heterogeneous Nucleation of P(VDF/TrFE)/PMMA Blends

PMMA Content (wt %)	$\gamma\gamma_e$ (erg^2/cm^4)	ΔG^* (kcal/mol) at ΔT = 20°C	ΔG_η (kcal/mol)[a] at ΔT = 20°C
0	217.36	7.47	8.46
10	185.35	6.35	8.84
15	224.49	7.68	9.06
20	226.92	7.75	9.29
25	231.37	7.87	9.58

[a] $\Delta G_\eta = C_1 RT/(C_2 + T - T_g)$, where $C_1 = 2078$ and $C_2 = 51.6$. $1/T_g = w_1/T_{g1} + w_2/T_{g2}$, where w_1 and w_2 are weight fraction of PMMA and P(VDF)/TrFE, respectively, and T_{g1} andf T_{g2} are glass transition temperature of PMMA and P(VDF/TrFE), respectively. (T_{g1} = 373 K and T_{g2} = 263 K).

The melting behavior of many polymers shows multiple (usually dual) melting endotherms.[7] The cause of this dual melting transition are generally interpreted to be one of the following: (1) melting, followed by recrystallization and final melting, and (2) melting of crystals with quite different crystalline morphology. It is not difficult to find out which effect is more significant in double melting by analyzing the DSC melting curves recorded at different heating rates. In the first case, the lower melting peak increases in intensity relative to the higher melting peak as the rate of scanning increases, be-

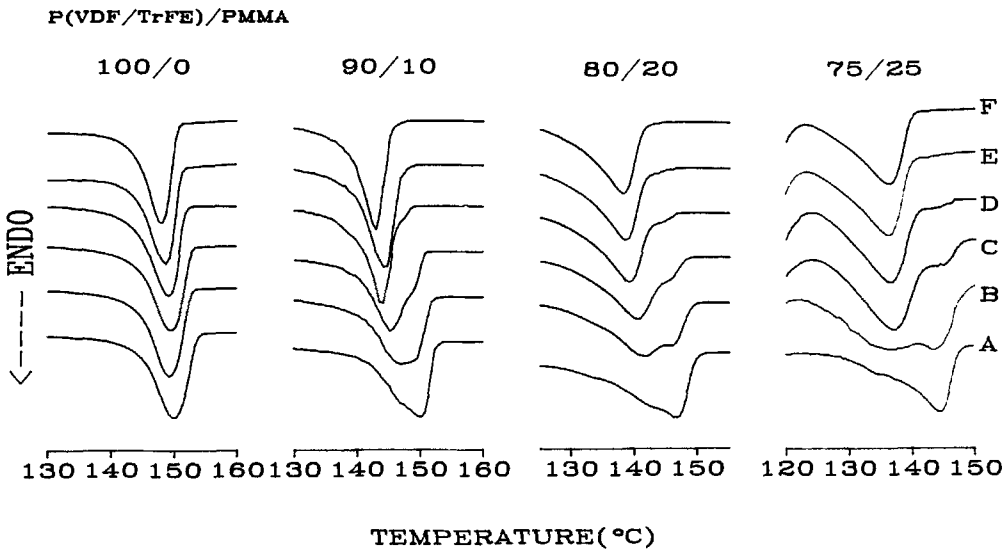

Figure 6 DSC thermograms of the P(VDF/TrFE)/PMMA blends crystallized nonisothermally at various cooling rates from the melt to 80°C upon heating at 10°C/min. Cooling rates for nonisothermal crystallization (°C/min): (A) 2, (B) 4, (C) 8, (D) 16, (E) 30, and (F) 60.

cause there is not enough time to reorganize or recrystallize at the higher rates of heating. In the second case, however, the relative intensities of two melting peaks are nearly constant irrespective of the rate of heating.

The samples of the P(VDF/TrFE)/PMMA blend, which were crystallized isothermally, did not show double melting endotherms, but double melting transition was observed for the nonisothermally crystallized blends. Figure 5 shows the melting endotherms recorded at various heating rates for the P(VDF/TrFE)/PMMA(80/20) blend crystallized nonisothermally from the melt to 10°C at −10°C/min. Since the relative size of the two melting endotherms is rarely changed at the various heating rates, the double melting of this blend is believed to be associated with the melting of two morphologically different crystals.

Figure 6 shows melting transition curves measured at the constant rate of heating of 10°C/min for each blend crystallized nonisothermally at various cooling rates. All the blends having more than 5 wt % of PMMA show distinct double melting behavior. As the cooling rate adopted in nonisothermal crystallization is reduced, the magnitude of the lower melting peak (T_{m1}) decreases relative to the higher temperature endotherm (T_{m2}) and both T_{m1} and T_{m2} are shifted to higher temperatures. As the concentration of PMMA increases in the blend, the gap between T_{m1} and T_{m2} increases. All the isothermally crystallized blend samples show a single melting transition regardless of the rate of heating. The crystals formed in isothermal crystallization have similar morphology. On the other hand, the nonisothermal crystallized samples are likely to have two morphologically different paraelectric crystals, one of which is more perfect and of greater lamellar thickness (form 1) and the other of which is less perfect and of thinner lamellar thickness (form 2). As discussed above, the increase of PMMA concentration increases T_g, reduces the diffusivity of crystallizable chain, and, consequently, inhibits crystal thickening and reduces the rate of crystallization. Therefore, the higher PMMA concentration produces greater morphological differences between the two crystal types.

CONCLUSION

Factor analysis and melting-point depression indicate miscibility between P(VDF/TrFE)/PMMA in the melt state. PMMA increases both ΔG^* and ΔG_η, which reduces the rate of crystallization drastically. Isothermally crystallized samples show a single melting transition, while nonisothermally crystallized samples exhibit a double melting transition that is attributed to morphologically different crystals present in the paraelectric crystalline phase. As the amount of PMMA increases, the morphological

difference becomes greater in the paraelectric crystalline phase formed through nonisothermal crystallization.

This work was supported by the Korea Science and Engineering Foundation (KOSEF) under grant KOSEF 901-1005-01201.

REFERENCES

1. T. S. Chow, *Macromolecules,* **23,** 333 (1990).
2. C. Léonard, J. L. Halary, and L. Monnerie, *Macromolecules,* **21,** 2988 (1988).
3. K. Saito, S. Miyata, T. T. Wang, Y. S. Jo, and R. Chujo, *Macromolecules,* **19,** 2450 (1986).
4. K. J. Kim and G. B. Kim, *J. Appl. Polym. Sci.,* **47,** 1781 (1993).
5. E. R. Malinowski, *Anal. Chem.,* **49,** 602, 612 (1977).
6. T. Nishi and T. T. Wang, *Macromolecules,* **8,** 909 (1975).
7. P. B. Rim and J. P. Runt, *Macromolecules,* **17,** 1520 (1984).
8. B. Wundlich, *Macromolecular Physics,* Academic Press, New York, 1976, Vol. 2, pp. 13, 27, 36–88, 162.
9. T. T. Wang and T. Nishi, *Macromolecules,* **10,** 421 (1977).

Received April 15, 1992
Accepted September 30, 1992